

Parametric Analysis of a TOUGH2 Model for the Unsaturated Zone at Yucca Mountain

Yanyong Xiang, Srikanta Mishra and Bryan Dunlap
CRWMS M&O/INTERA, Inc.
101 Convention Center Drive, Suite P110
Las Vegas, NV 89109

1. BACKGROUND AND SCOPE

Yucca Mountain in Nevada is currently being investigated for suitability as a potential site for the disposal of high-level radioactive waste and spent nuclear fuel. As the most important natural barrier against radionuclide migration to the accessible environment, the unsaturated zone at Yucca mountain is a key constituent in assessing the ambient geohydrology. A three-dimensional site-scale TOUGH2 model of the unsaturated zone is currently under development by Lawrence Berkeley Laboratory (LBL) and the United States Geological Survey (USGS) (*Wittwer et al.*, 1993; *Bodvarsson et al.*, 1994). The model covers an area of about 30 km² (**Figure 1**), and consists of six hydrogeologic units - TCw (Tiva Canyon welded), PTn (Paintbrush nonwelded), TSw (Topopah Spring welded), TSv (Topopah Spring welded-vitrophyre), CHnv (Calico Hills nonwelded-vitric), and CHnz (Calico Hills nonwelded-zeolitic), which are further subdivided into seventeen layers to represent additional lithologic detail (**Table I, Figure 2**). Based on the work of *Klavetter and Peters* (1986), the fractured units TCw and TSw are treated as equivalent continua with specified threshold saturations for triggering fracture flow.

Using two northwest to southeast cross sections (one including the Ghost Dance fault, and the other including the Abandoned Wash and Dune Wash faults), *Wittwer et al.* (1993) investigated the impacts of two extreme (high, low) fault permeabilities on moisture flow patterns. Their analyses indicated that steady-state moisture flow is dominantly vertical, whereas marginal lateral flow occurs only in some localized regions where prominent dipping stratigraphy and contrasting permeabilities exist. The three-dimensional analyses by *Bodvarsson et al.* (1994), who assumed three hydrological representations of the faults, i.e., capillary barrier, low permeability, and high permeability, indicated complex lateral as well as vertical flow patterns.

Further evaluation of the effects of input uncertainty (i.e., hydrologic representation of rock units and infiltration rate/pattern imposed at the ground surface) on predictions of the site-scale model are presented in this paper. These simulations are intended to help understand the range of expected system response subject to various uncertainties, and as such provide the bases for developing the abstractions of the ambient unsaturated flow regime for incorporation in total system performance assessment models. An associated objective is to examine the geometry of flow paths predicted by multidimensional models in order to substantiate the assumption of one-dimensional flow paths conventionally used in total system models.

2. MODEL DESCRIPTION

2.1 Geometry and Boundary Conditions

The simulations discussed herein are based on a northwest-southeast cross-section of Yucca Mountain (Figure 2) which is extracted from the LBL-USGS 3-D site-scale model. The cross-section passes through the potential repository area and includes the Ghost Dance Fault. The left and right boundaries are assumed to be of the no-flow type. The top boundary (ground surface) is treated as a constant pressure/temperature single-phase air surface. The bottom boundary (water table) is treated as essentially a single-phase liquid surface (a liquid saturation of 0.999) at constant pressure and temperature. Both top and bottom boundary conditions are imposed via fictitious grid blocks of large volumes with their nodal points placed on the physical boundaries. Infiltration at the ground surface is simulated as liquid sources located at the nodal points of the top layer grid blocks. Note that the constant pure-air condition at the ground surface precludes any possibility of moisture flow above the mountain, and that the water table boundary condition implies that the saturated zone acts as a sink of infinite capacity.

2.2 Parametrization

The original LBL-USGS site-scale model uses a 'best-guess' hydrologic parameter set (Wittwer *et al.*, 1993). An alternative set of material properties has been presented as part of a Performance Assessment Data Base developed at Sandia National Laboratories (Wilson *et al.*, 1994). This data set includes ranges and summary statistics associated with each hydraulic property (porosity, saturated permeability, and Van Genuchten parameters) for all hydrogeologic units, and as such, is more amenable to uncertainty propagation studies. Note that the SNL data are organized with respect to the six major hydrogeologic units, whereas the LBL data correspond to a more detailed stratigraphy to represent modest intra-unit changes in hydrogeologic properties. To examine the impacts of such a detailed representation of rock units (or the lack thereof) on the hydrologic behavior of the system, the original 17-layer LBL data were reduced to a 6-layer parameter set by averaging the various parameters within each of the six major units. Geometric averaging was used for saturated permeability and the Van Genuchten air-entry scaling parameter, and arithmetic averaging was used for porosity and the Van Genuchten pore-size distribution parameter. Table I presents a comparison of the original LBL data, the averaged LBL data, and the SNL data. Note that both matrix and fracture residual saturations are assumed to be zero in LBL data, and are assumed to take the following values in the SNL data: TCw - 0.021, PTn - 0.154, TSw - 0.045, TSv - 0.118, CHnv - 0.097, and CHnz - 0.121.

3. RESULTS AND DISCUSSION

3.1 Sensitivity to Matrix Properties

Figure 2 shows the model discretization along with a color image of the liquid saturation distribution for a constant infiltration rate of 0.1 mm/yr with the original LBL parameters. Picking column 153 as a representative column of the two-dimensional system within the proposed repository region, Corresponding to the infiltration rates of 0.0 mm/yr and 0.1 mm/yr, respectively, Figures 3 and 4 show liquid saturation profiles for the LBL and SNL data sets. As

expected, the average LBL property case is a more smeared version of the response obtained with the original LBL data set. Both the original and the averaged LBL data sets produce liquid saturations in the nonwelded (PTn and CHnv) units much higher than those from the SNL data, although the predicted saturations agree much better for the welded (TCw, TSw and TSv) units. The liquid distribution patterns shown in **Figure 3** primarily reflect differences in capillary properties of the different units as defined in the various data sets. Note that increasing the infiltration rate reduces the differences between the three data sets in predictions of liquid saturations in the welded units. **Figures 5 and 6** are plots of liquid-phase velocity fields and streamlines corresponding to the original LBL and the averaged LBL data, respectively. Lateral flow is seen to occur along the interfaces between TCw and PTn, and between TSv and CHnv, which coincide with sharp permeability contrasts. The lateral flow is also enhanced, due to gravity, by the eastward dipping stratigraphy of all units. The lateral flow for the averaged LBL data is of a much smaller extent than for the original LBL data.

Figure 7 describes vertical linear liquid velocity distributions along column 153. Note that all three different hydrologic descriptions assume essentially the same velocity distribution pattern, although abrupt velocity variations occur at unit interfaces. **Figure 8** plots the liquid-phase particle travel times from ground surface to the water table, as a function of infiltration rate, assuming vertical flow only along columns 153, 157, and the Ghost Dance Fault. It indicates that the fault of distinctively higher permeability is the fastest travel path, and that the three columns resemble one another in travel time as a function of infiltration rate. The finite velocities observed for the zero infiltration case are an artifact of the vertical liquid-vapor counterflow induced by the geothermal gradient and by the fixed pure-air assumption for the top boundary.

3.2 Sensitivity to Fracture Properties

As described in *Klavetter and Peters* (1986) and *Wittwer et al.* (1993), a threshold saturation has been used as the pivoting parameter above which fluid flow occurs in the fracture as well as in the matrix. In the simulations described above, such composite fracture-matrix models have been used to represent the fluid transmitting properties of the welded units, assuming a fracture porosity of 0.001. To examine the sensitivity of liquid saturation distributions to the assumptions regarding the composite model fracture porosity values, simulations are conducted using different fluid transmission models and fracture porosities. **Figure 9** indicates that for all the three data sets, the liquid saturations for the composite model are only fractionally smaller than those for the matrix-only model in the welded units, whereas no difference exist in other units. **Figure 10** describes the liquid distributions along column 153 using the composite matrix-fracture model with different fracture porosity values. The liquid saturations in the welded units for the 0.005 fracture porosity case are apparently smaller, but still by insignificant magnitudes.

3.3 Sensitivity to Imposed Patterns of Infiltration

Another source of uncertainty is related to the specification of infiltration patterns and intensities at the ground surface, which are dependent upon the moisture transmitting properties of the surficial materials and climatic conditions. It is also necessary to estimate the depth at which seasonal fluctuations diminish and steady-state downward flux conditions are likely to occur. By assuming exclusive matrix flow and relating infiltration to the estimated hydraulic properties of the surficial materials, *Flint and Flint* (1994) proposed a distributed infiltration map for the LBL

three-dimensional unsaturated zone model, ranging from 0.02 mm/yr for TCw to 13.4 mm/yr for PTn. **Figure 11** shows the liquid-phase velocity field and the streamlines corresponding to a 10.0 mm/yr infiltration rate for the PTn outcrop at the top-left corner and a 0.1 mm/yr rate for other areas. Comparing **Figure 11** with **Figure 5**, and examining **Figure 12**, it can be observed that the higher infiltration only has appreciable effects localized in the vicinity of the PTn outcrop.

4. CONCLUDING REMARKS

The hydrologic effects of different matrix/fracture properties and infiltration patterns on ambient (steady-state) unsaturated flow at Yucca Mountain have been examined using a series of two-dimensional cross-sectional simulations. The major findings can be summarized as follows:

- (1) The SNL data set produces much lower liquid saturations than the LBL data sets for the non-welded units. Averaging of the original LBL data has smearing effects on liquid distributions and reduces the extent of lateral flow. At higher infiltration rates, the differences in liquid distributions in the welded units between the three data sets diminish.
- (2) Liquid flow is vertically dominant in most regions, while lateral liquid flow is of much smaller magnitude and induced mainly by the nonwelded units due to their distinctively higher permeabilities, and by the eastward dipping stratigraphy.
- (3) Vertical continuity of liquid along a column can be assumed without inducing significant errors in estimating liquid-phase particle travel times.
- (4) Saturations predicted for the welded units by the composite-porosity model, with a fracture porosity of 0.001, are only marginally smaller than those for a matrix-only flow model. Increasing the fracture porosity by a factor of five produces only a small decrease in saturation for the welded units.
- (5) Locally focussed infiltration can enhance lateral flow, but such effects diminish for more distant regions.

The results presented in this paper were derived from simulations based on various simplifications and assumptions. Future work should be directed toward describing the ambient unsaturated zone hydrology in greater detail, e.g., better representation of the interfaces between the unsaturated zone and the water table/atmosphere, consideration of the variabilities in material properties and their most probable combinations, incorporation of alternate conceptual models for non-equilibrium fracture-matrix interaction.

5. REFERENCES

Bodvarsson, G., et al., Preliminary analysis of three-dimensional moisture flow within Yucca Mountain, Nevada, *High Level Radioactive Waste Management, Proceedings of the Fifth Annual International Conference, Las Vegas, 2038-2047, 1994*

Flint, A., and L. E. Flint, Spatial distribution of potential near surface moisture flux at Yucca Mountain, *High Level Radioactive Waste Management, Proceedings of the Fifth Annual International Conference, Las Vegas, 2352-2358, 1994*

Klavetter, E. A., and R. R. Peters, Estimation of hydrologic properties of an unsaturated fractured rock mass, SAND84-2642, Sandia National Laboratories, 1986.

Wilson M. L. et al., Total-system performance assessment for Yucca Mountain-SNL second iteration (TSPA-1993), SAND93-2675, 1994.

Wittwer, C. S., et al., Studies of the role of fault zones on fluid flow using the site-scale numerical model of Yucca Mountain, *High Level Radioactive Waste Management, Proceedings of the Fourth Annual International Conference, Las Vegas, 667-674, 1993.*

Table I. Stratigraphy and Hydrologic Properties
(LBL—original LBL data, AVE.—averaged LBL data, SNL—SNL data)

Unit	Layer	Porosity (%)			Pemeability (m ²)			VG α (10 ⁻⁵ Pa ⁻¹)			VG β		
		LBL	AVE.	SNL	LBL	AVE.	SNL	LBL	AVE.	SNL	LBL	AVE.	SNL
TCw	11	17			1e-18			0.067			1.33		
	12	17	13	9	2e-18	1.0e-18	1.3e-18	0.067	0.067	0.081	1.33	1.333	1.608
	13	6			1e-18			0.067			1.33		
PTn	21	33			1e-13			1.67			1.20		
	22	37	34	42	5e-14	7.9e-14	1.1e-15	6.0	3.5	0.74	1.19	1.186	2.222
	23	32			1e-13			4.33			1.17		
TSv	31	6	6	7	1e-18	1.0e-18	1.0e-18	0.067	0.067	0.024	1.41	1.408	2.232
TSw	32	15			4e-16			0.125			1.22		
	33	13	14	14	4e-18	1.4e-17	2.0e-18	0.2	0.12	0.13	1.28	1.290	1.709
	34	14			5e-18			0.133			1.33		
	35	12			5e-18			0.067			1.33		
TSv	36	5	6	7	1e-18	1.0e-18	1.0e-18	0.067	0.067	0.024	1.41	1.408	2.232
CHnv	51	35			2e-13			2.0			1.15		
	52	28	34	33	3e-13	2.6e-13	1.0e-16	2.0	2.0	0.23	1.14	1.140	2.358
	53	39			3e-13			2.0			1.14		
CHnz	54	25			1e-16			0.1			1.23		
	55	25	25	31	1e-16	1.0e-16	1.6e-18	0.1	0.1	0.054	1.23	1.235	1.672

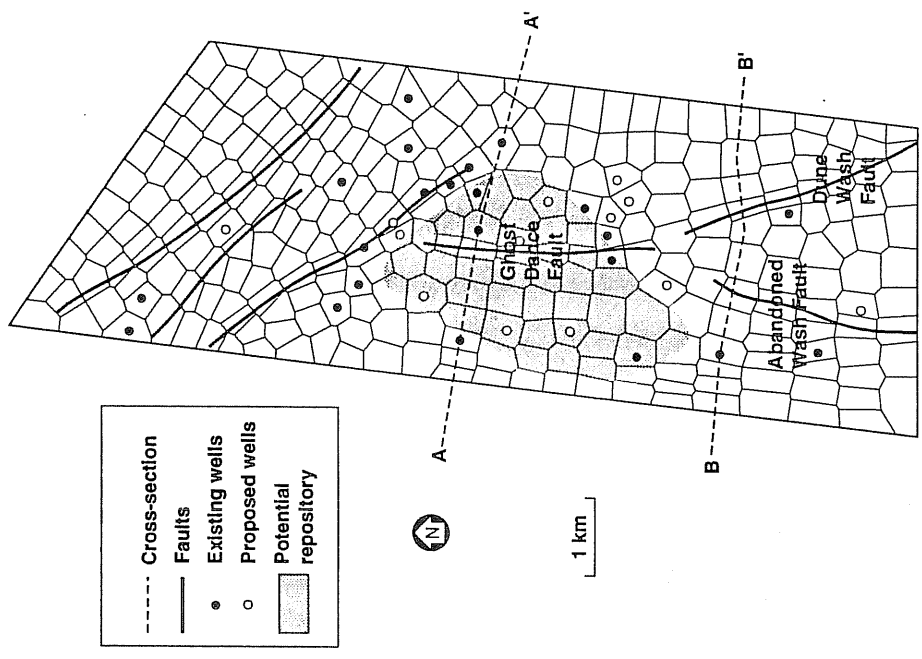


Figure 1: Horizontal grid of the LBL-USGS model, showing locations of the two cross sections.

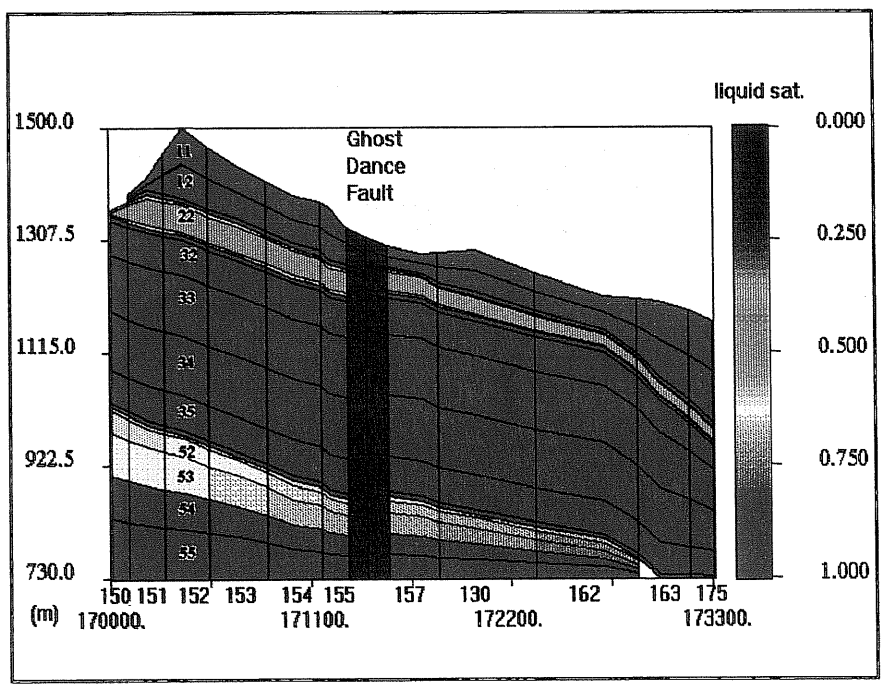


Figure 2: Discretization and stratigraphy of the cross section A-A', with the color image representing the liquid distribution under the original LBL description and a uniform infiltration of 0.1 mm/year.

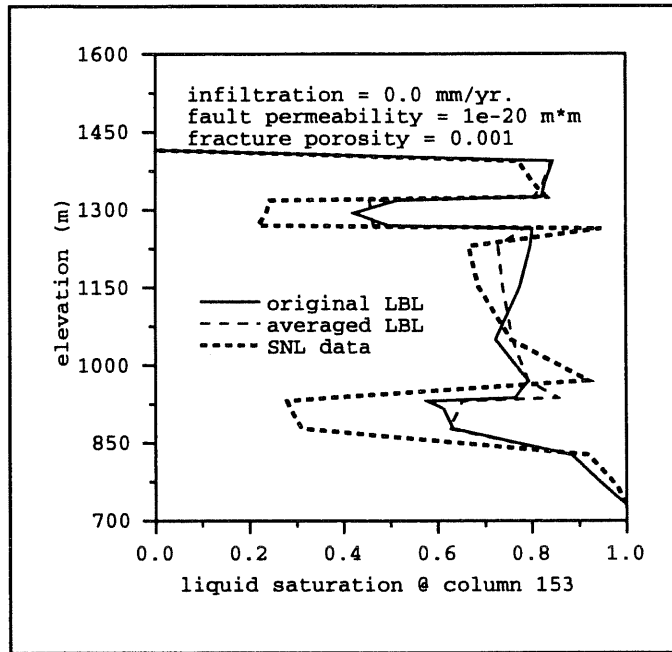


Figure 3: Liquid distributions along column 153 under an infiltration rate of 0.0 mm/year.

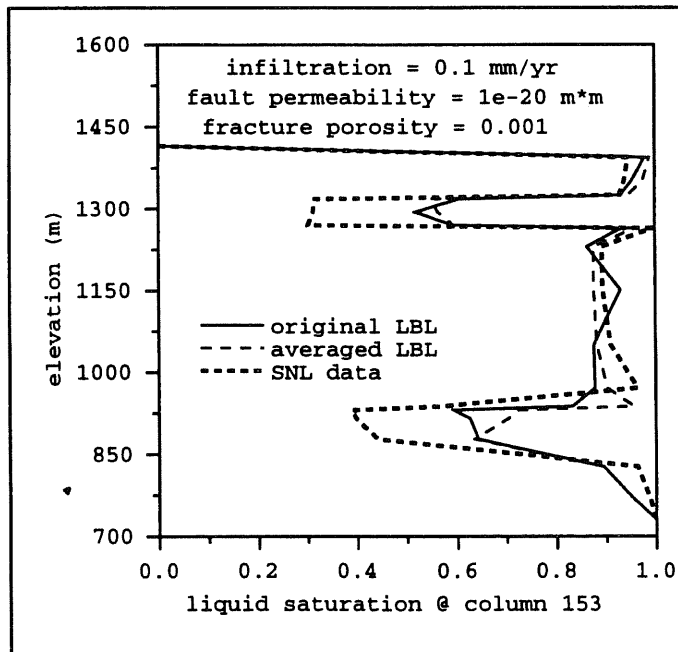


Figure 4: Liquid distributions along column 153 under an infiltration rate of 0.1 mm/year.

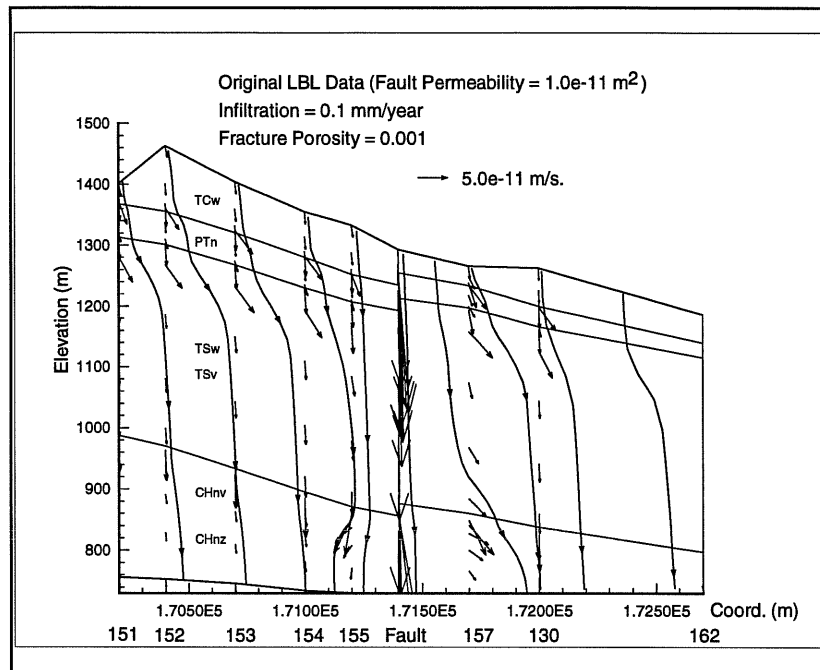


Figure 5: Liquid phase velocity field and streamlines under the original LBL description and a uniform infiltration of 0.1 mm/year.

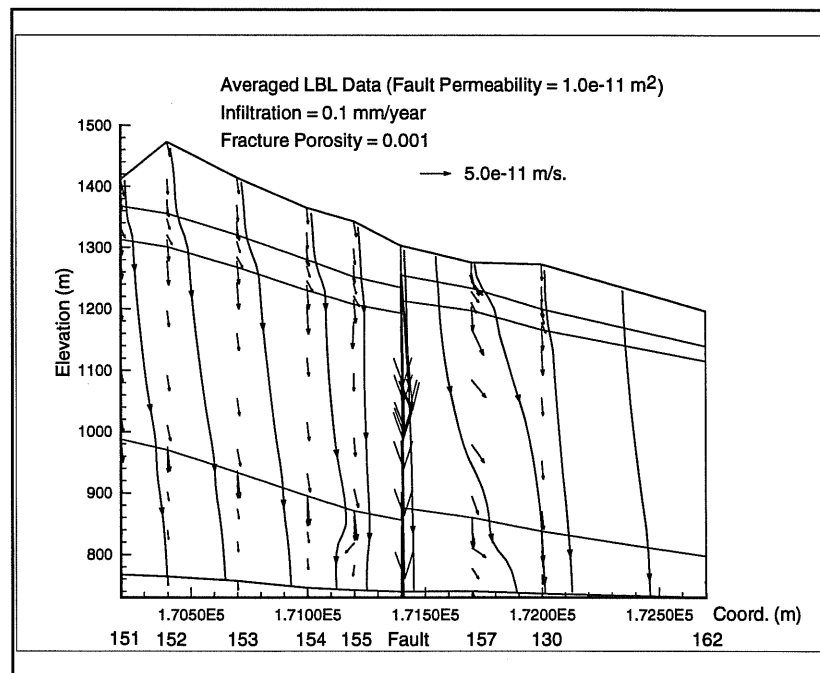


Figure 6: Liquid phase velocity field and streamlines under the averaged LBL description and a uniform infiltration of 0.1 mm/year.

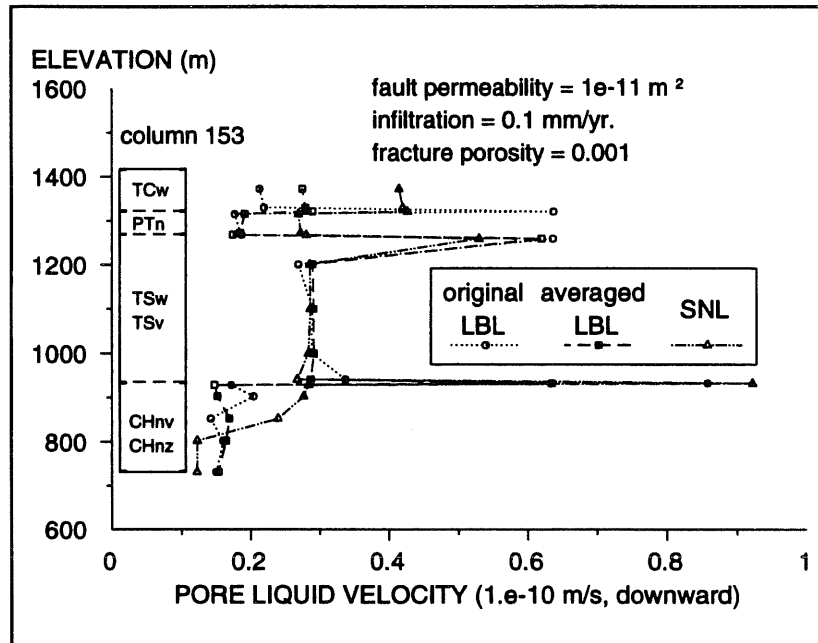


Figure 7: Vertical liquid phase linear velocity distributions along column 153.

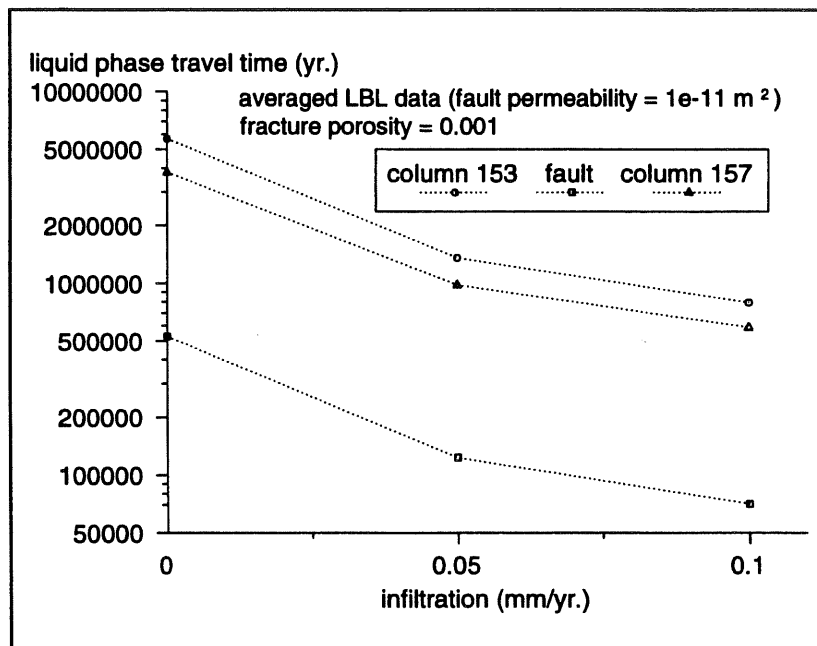


Figure 8: Estimated particle travel time in liquid phase as a function of infiltration rate,

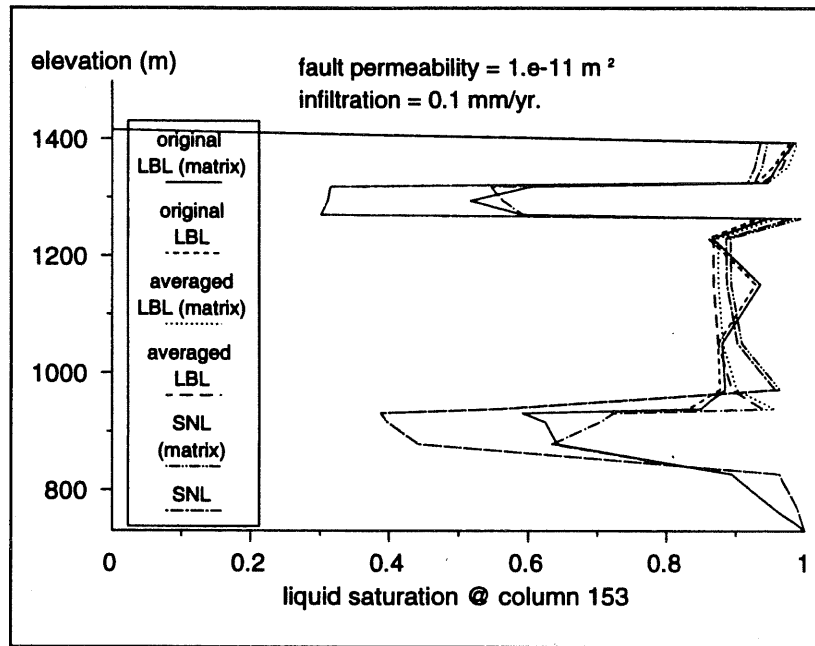


Figure 9: Liquid distributions along column 153 for matrix-only and composite matrix-fracture flow models.

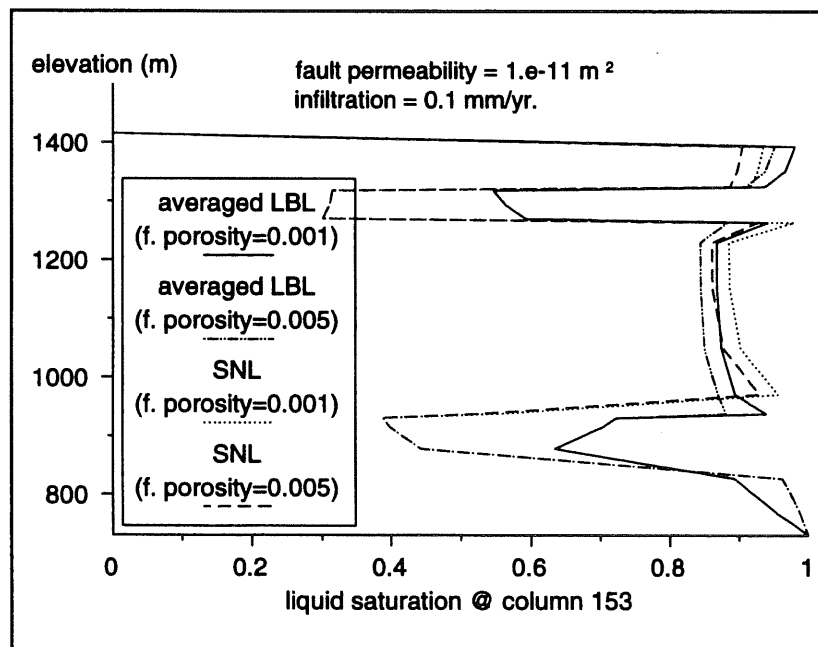


Figure 10: Liquid distributions along column 153 for different fracture porosity values.

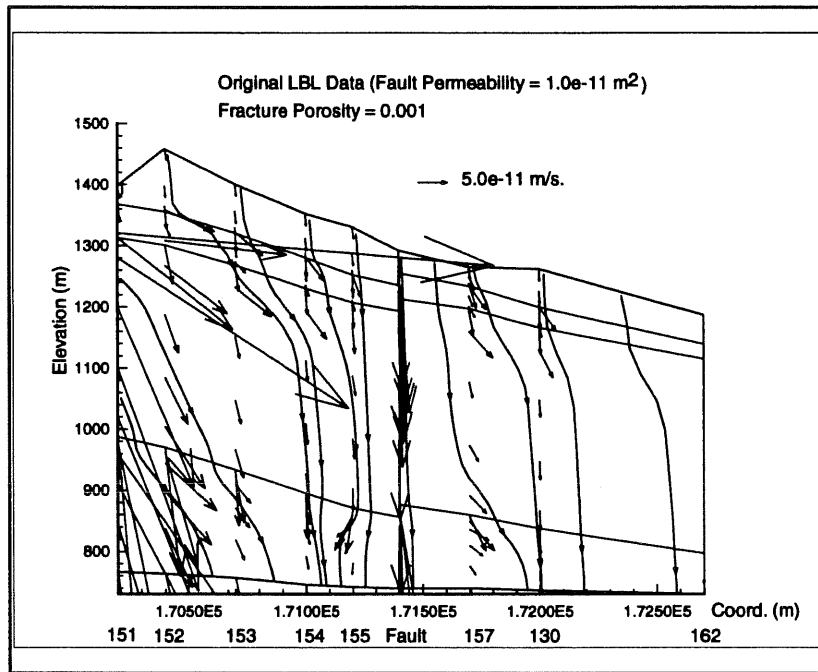


Figure 11: Liquid Phase velocity field and streamlines under the original LBL description and infiltration of 10.0 mm/year for the PTn outcrop and 0.1 mm/year for other areas.

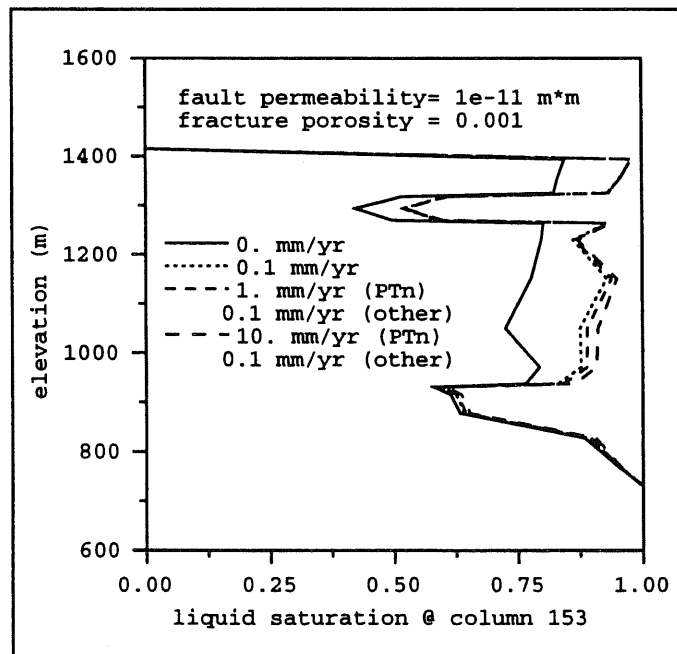


Figure 12: Liquid distributions along column 153 under the original LBL description and various infiltrations.